# Comparative proteomics uncovers correlation between tRip-mediated host tRNA import and asparagine insertion in *Plasmodium* proteins.

Martina Pitolli[a], Marta Cela[a1], Delphine Kapps[a], Johana Chicher[b], Laurence Despons[a] and Magali Frugier[a*]

[a]Université de Strasbourg, CNRS, Architecture et Réactivité de l'ARN, UPR 9002, F-67084 Strasbourg, France

[b]Strasbourg-Esplanade Proteomics facility, Université de Strasbourg, F-67084 Strasbourg, France.

[1]present address: Molecular Microbiology and Structural Biochemistry, CNRS UMR 5086, Université Claude Bernard Lyon 1, Lyon, France

*to whom correspondence should be addressed: Email: m.frugier@ibmc-cnrs.unistra.fr

**Authors Contributions**: MP, DK and MC performed experiments, data acquisition, and analysis, JC performed mass spectrometry analysis and LD provided computer programming. MF managed the conception, design, interpretation of data and funding acquisition and wrote, reviewed, and edited the manuscript.

**Competing Interest Statement**: The authors declare no conflict of interest.

**Classification:** Biochemistry

**Key words:** tRNA, translational control, proteomics, amino acid usage

**This PDF file includes:**

Main Text, Figures 1 to 4, and supporting information.

## Abstract

tRNAs are not only essential for decoding the genetic code, but their abundance also has a strong impact on the rate of protein production, folding, and on the stability of their encoding messenger RNAs. *Plasmodium* expresses a unique surface protein called tRip, involved in the import of exogenous tRNAs into the parasite. Comparative proteomic analysis of the blood stage of wild-type and tRip-KO variant of *P. berghei* parasites revealed that down-regulated proteins in the mutant parasite are distinguished by a bias in their asparagine content. We therefore propose a model in which a dynamic import of host $tRNA^{Asn}$ allows the synthesis of asparagine-rich regulatory proteins that efficiently and selectively control the parasite infectivity. These results suggest a novel mechanism of translational control where import of host tRNAs emerge as critical regulator of gene expression in the *Plasmodium* developmental cycle and pathogenesis.

## Significance Statement

tRip is a surface protein involved in the import of exogenous tRNAs into the malaria parasite, *Plasmodium*. To better understand tRNA import and protein synthesis in *Plasmodium*, the proteomes of wild-type and tRip-KO parasites were compared. Most of the proteins deregulated in the tRip-KO parasite were under expressed compared to the wild-type. Asparagine usage was greatly increased in the proteins that were down-regulated in the tRip-KO, suggesting that the mutated parasite is impaired in inserting asparagine into proteins. Moreover, the presence of host tRNAs inside the blood stage parasite and the possibility of charging these imported tRNAs with endogenous aminoacyl-tRNA synthetases, led us to propose that, imported host tRNAs participate in parasite protein synthesis and control its development.

## Introduction

We have discovered the only example to date of an exogenous tRNA import pathway, summarized in Figure 1 (1–4). In *Plasmodium*, the malaria parasite, *P. berghei* sporozoites (the extracellular infective form of the parasite, Figure S1) isolated from the salivary glands of infected mosquitoes import exogenous tRNAs *via* a surface protein, named tRip (tRNA import protein). However, the absence of homologous mechanisms in other organisms raises the question of the role of this unique tRNA import and its mode of action. It has been established that (i) tRip is a homodimeric protein made of an N-terminal GST-like domain and a C-terminal EMAPII-like tRNA binding domain; (ii) tRip binds human tRNAs with high affinity *in vitro* and with a stoichiometry of one tRNA per tRip dimer; (iii) tRip is located on the parasite surface with its tRNA binding domain exposed to the host system; (iv) immunolocalization experiments found tRip expressed both in the liver and blood stages in the vertebrate host, as well as in the intestine and salivary glands of the mosquito; (v) *in vitro*, exogenous tRNAs enter living sporozoites; (vi) the knockout parasite, tRip-KO, does not import tRNAs, its protein biosynthesis is significantly reduced, and its growth is decreased in vertebrate blood compared to the wild-type parasite.

Recently, the crystal structure of the dimeric N-terminal GST-like domain of *P. vivax* tRip was solved and revealed a unique homodimerization interface (5). We confirmed by SAXS that this unusual interface exists in solution and that it allows Multi-Synthetase Complex (MSC) formation (3, 4). Indeed, three aminoacyl-tRNA synthetases (aaRS), namely glutamyl- (ERS), glutaminyl- (QRS) and methionyl- (MRS) tRNA synthetases, specifically co-immunoprecipitate with tRip; These enzymes all contain an N-terminal GST-like domain involved in MSC assembly. Unexpectedly, these proteins form two exclusive heterotrimeric MSCs with a 2:2:2 stoichiometry: a Q-complex (tRip:ERS:QRS) and an M-complex (tRip:ERS:MRS) characterized by different biophysical properties and interaction networks (Figure 1). We could also identify a set of host tRNAs preferentially bound by tRip and potentially best imported into the parasite. Interestingly, tRip does not bind to tRNAs in a sequence-dependent manner, but rather recognizes post-transcriptional modifications that modulate this interaction (2). In contrast to what was found with the cytosolic yeast Arc1p (6), the tRNAs that best bind tRip do not correspond to the aaRSs that compose the two MSCs, suggesting that, although tRip is an aminoacyl-tRNA synthetase interacting multifunctional protein (AIMP), it is not dedicated to the aminoacylation of specific tRNAs (2), thereby

leading us to search for a novel function for this unique membrane protein and the tRNA import with which it is associated.

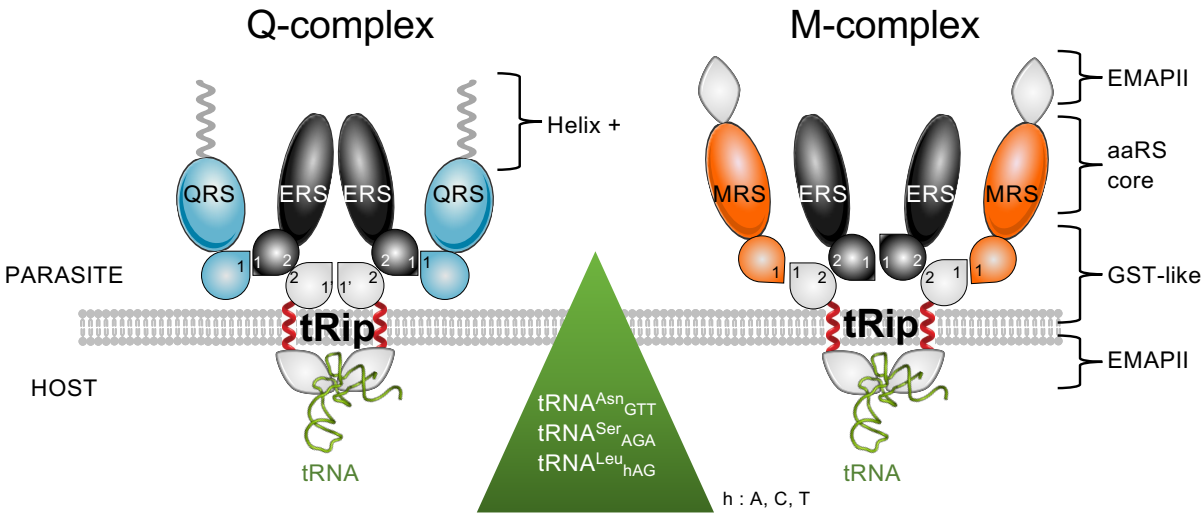


**Figure 1: *P. berghei* membrane-bound multi-synthetase complexes.** *Plasmodium* is characterized by the presence of two multisynthetase complexes (MSC) named Q-complex and M-complex. The Q-complex is composed of glutamyl- (ERS) and glutaminyl- (QRS) tRNA synthetases linked to a dimer of tRip whereas the M-complex is composed of tRip and Methionyl-tRNA synthetase (MRS) organized around a dimer of ERS. tRip is therefore an AIMP (Aminoacyl-tRNA synthetase Interacting Multifunctional Protein). tRip, ERS, QRS, and MRS are schematized and colored in grey, black, cyan, and orange, respectively. the GST-like domains are shown as a drop and the C-terminal domains of tRip, QRS and MRS involved in tRNA binding are either EMAPII-like domains (tRip and MRS, grey diamonds) or a positively-charged $\alpha$-helix (QRS, shown as a grey helix). The characteristic feature of *Plasmodium* MSCs is that tRip is a membrane protein (the transmembrane helix is shown in red) with the GST-like domain required for MSC formation localized inside the parasite and the tRNA binding domain exposed outside the parasite to host tRNAs. This unique organization justifies that only the EMAPII-like domain of tRip ($tRip_{200-402}$) is fused at the C-terminal domain of a GST domain and used as a target for the selection of aptamers capable of inhibiting tRip tRNA binding. Interfaces 1, 1' or 2, involved in protein-protein interactions, are indicated in the corresponding GST-like domains.

Interestingly, tRip is not the only protein that has been characterized as cytosolic in other organisms and is actually localized on the surface of *Plasmodium*. This is also the case for other RNA-binding proteins such as the poly-A binding protein-1 (PABP-1) (7) and the glyceraldehyde-3 phosphate dehydrogenase (GAPDH) (8), which are both found on the surface of the sporozoite. The presence of different RNA-binding proteins at the parasite-host interface is another indication that RNA

exchange might control unsuspected host-parasite interactions that take place during the parasite life cycle. In the present study, we compared the proteomes of the wild-type (WT) and the tRip-KO blood stage parasites with the objective of understanding the fate of imported tRNAs in *Plasmodium* protein synthesis and its infectious process.

## Results

**Quantitative proteomics of tRip-KO *versus* wild-type (WT) schizonts.** We investigated the relative protein abundance of tRip-KO *versus* WT in the schizont stage of synchronized parasites (Figure S1) using liquid chromatography coupled to tandem mass spectrometry (LC-MS/MS) and a label-free quantification method. Three biological replicates for tRip-KO and WT were defined for the schizonts samples (Table S1). The proteomic data sets (KO and WT) were considered comparable as most proteins were stable. This is notably the case for four constitutively expressed proteins: EF1-$\alpha$ (PBANKA_1133300), Hsp70 (PBANKA_0914400), enolase (PBANKA_1214300) and histone H4 (PBANKA_941900) (Table S1). Protein abundance was calculated using the intensity of *P. berghei* peptides, which identified between 347 and 469 proteins. Metric multidimensional scaling (MDS) (included in Table S1) indicated clustering of the tRip-KO and WT parasites, suggesting there are distinct groups of differentially abundant proteins between the two genotypes. Among these proteins, only 8 were significantly up-regulated and 49 were down-regulated in the tRip-KO parasites compared to the WT (*p-value* $< 0.05$) with a at least a 2-fold change in abundance; they are highlighted in the volcano plots in orange and green, respectively (Figure 2A). Most of down-regulated proteins are involved in translation (31% ribosomal proteins, initiation, and elongation factors); the two other abundant categories were surface proteins involved in transport and invasion (16%) and proteins with unknown functions (14%) (Table S1).

**Amino acid compositions of tRip-KO down-regulated proteins.** Amino acid utilization in the 100 most expressed stable proteins was compared with that of the significantly down-regulated proteins in the tRip-KO parasite (Figure 2B). There is a 70% increase in asparagine in the proteins down-regulated in the tRip-KO parasite compared to the wild-type (Table S2, 11.6% in tRip-KO *versus* 6.8% in WT), thus, suggesting that the tRip-KO parasite has difficulty translating asparagine-rich proteins.

**Quantitative proteomics of tRip-KO *versus* WT in "Blood stages" samples.** Three biological replicates for tRip-KO and WT containing all blood stages (rings, trophozoites, and schizonts) were used

for comparative proteomics (Figure S1, Table S3). Triplicate proteomic data sets (KO and WT) were compared and identified between 617 and 1017 proteins each time. Sixty-nine proteins were significantly deregulated (at least a 2-fold change in abundance), 8 were up-regulated and 61 were down-regulated in the tRip-KO parasites compared to the WT (*p-value* < 0.05) (Figure 2C). The few up-regulated proteins are especially rhoptry associated proteins (a specialized organelle in *Plasmodia*) and proteins involved

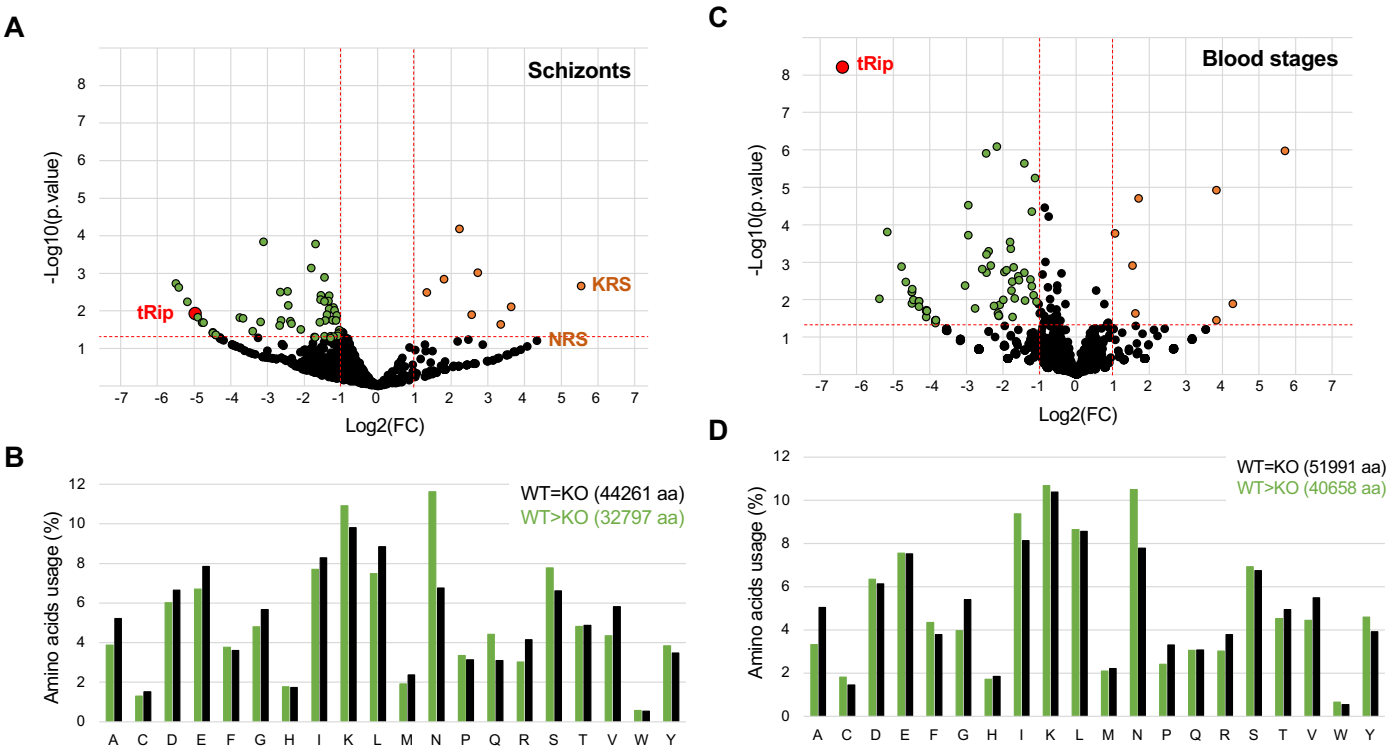


**Figure 2: Comparative proteomic analysis and amino acid usage of proteins identified in WT and tRip-KO samples containing schizonts (A and B) or all blood stages (C and D).** (**A**) Volcano plot of all quantified proteins from WT and tRip-KO parasites displaying the relationship between statistical significance (−log10(*p-value*), y-axis) and log fold change (FC) of each protein (log2(FC), x-axis). Statistics are based on three independent experiments (Table S1). Deregulated proteins in tRip-KO parasite compared to the WT parasite are shown in orange (up-regulated, FC≥2 and *p-value* ≤ 0.05) and green (down-regulated, FC≤-1 and *p-value* ≤ 0.05). tRip is shown in red and black dots represent proteins with no significant change. KRS and NRS correspond to Lysyl- and asparaginyl-tRNA synthetases. (**B**) Comparison of amino acid usage (%) of proteins whose expression is stable in the tRip-KO parasite (the 150 most expressed proteins, black) and all proteins that are down-regulated in the tRip-KO parasite (green). Amino acids are designated by their one letter symbol and the total number of amino acids used in the analyses is specified. (**C**) Volcano plot of all quantified proteins from WT and tRip-KO parasites. Statistics are based on three independent experiments (Table S3). (**D**) Comparison of amino acid usage (%) between proteins whose expression is stable in the tRip-KO parasite (the 100 most expressed proteins, black) and proteins down-regulated in the tRip-KO parasite (green).

in mobility and invasion (Table S3), while down-regulated proteins were distributed across different functional families: Apart from the 20% of proteins with unknown function, most are involved in DNA replication (41%). Yet, none were common to the schizonts samples (compare Tables S1 and S3). Amino acid usage in the tRip-KO down-regulated proteins shows also that these proteins contain more asparagine residues (10.5% in tRip-KO *versus* 7.8% in WT) than the 150 most expressed stable proteins (Figures 2D, Table S2), leading to the same conclusion as above: in the absence of tRip, asparagine-rich proteins are less efficiently translated.

The mRNAs encoding 3 up- and 3 down-regulated proteins were quantified by qRT-PCR. While the mRNAs for the up-regulated proteins were not significantly affected, the mRNAs of the down-regulated proteins all showed a strong decrease in the tRip-KO parasite compared with the WT parasite (Figure S2, Table S4). Decreased translation of these mRNAs likely favors their rapid degradation, suggesting that down-regulated proteins are controlled at the level of mRNA stability.

**Identification of asparagine-rich proteins in *Plasmodia* strains.** Since both "schizonts" and blood stages samples strongly suggest that the tRip-KO parasite is hindered in inserting asparagine into proteins, the complete proteomes of six *Plasmodium* lineages (*P. falciparum*-5476 proteins, *P. berghei*-5076 proteins, *P. yoelii*-6097 proteins, *P. chabaudi*-5222 proteins, *P. knowlesi*-5340 proteins and *P. vivax*-6708 proteins) as well as *Toxoplasma gondii* (control, 8322 proteins) were retrieved from ApiDB (9) and analyzed for their asparagine content (Figure S3A). *Plasmodium* proteins contain more asparagine residues than *Toxoplasma*. Yet, the *P. knowlesi* and *P. vivax* proteomes contain fewer asparagine residues (an average of about 8 %) than the 4 other *Plasmodia* strains (average of about 12%) (Figure S3A, Table S2). Proteins were then ranked from highest to lowest asparagine contents to identify those that might be impacted by decreased asparagine decoding efficiency. For all proteomes, only the top 0.5% proteins were considered to identify conserved proteins containing the highest asparagine content. Depending on the strain, 25 to 30 proteins were selected (Table S5). This list includes 2 proteins that are strictly concerved in all strains and different members of AP2 domain transcription factors in all strains except *P. vivax*; The two ubiquitous proteins correspond to the CCR4-associated factor-1 (CAF-1) and the poly-A binding protein-3 (PABP-3). They share a particular modular organization with an N-terminal domain of high complexity and a low complexity C-terminal domain with a very high asparagine content (Figure S3B, C). The proportion of asparagine varies locally between 35 and 60% in *P. falciparum*, *P. yoelii*, *P. chabaudi* and *P. berghei* and between 20 and 25% in *P. knowlesi*

and *P. vivax*. But these two proteins are only detected by a few spectral counts in the proteomic data (Tables S1 and S3) which are therefore not usable.

**Comparison of tRip-KO and ΔC-CAF-1 phenotypes.** The *Plasmodium* CAF1 N-terminal domain is highly conserved in eukaryotes while the additional asparagine-rich C-terminal domain is found only in *Plasmodia.* The deletion of this *Plasmodium*-specific C-terminal domain results in overexpression of mRNAs encoding proteins involved in parasite egress and invasion (10): of the 19 *P. falciparum* mRNAs up-regulated in this ΔC-CAF-1 mutant (10), 8 of the corresponding proteins can be detected in the present study (all blood stages) (Figure 3): proteins essential for merozoite formation and entry into and exit from erythrocytes, such as the rhoptry proteins, RAP1, RAP2/3 and the major surface proteins AMA-1 and MSP1 (LogFC = 1.26, *p-value* = 0.078) are up-regulated in the tRip-KO proteome and their mRNA levels vary similarly in the ΔC-CAF-1 mutant (10). Another protein associated with merozoite invasion of erythrocytes (RON2) is up-regulated only in the tRip-KO parasite. However, the 3 other proteins GAP50, RhopH2 and RhopH3, encoded by up-regulated mRNAs in ΔC-CAF-1 (10) show no variation between the tRip-KO and the WT proteomes.

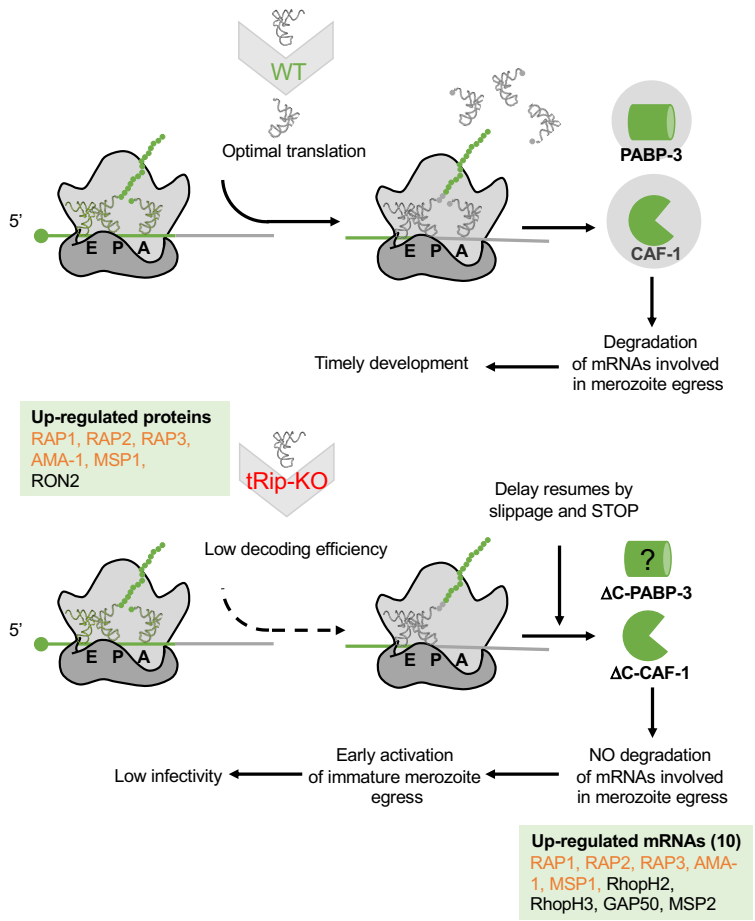


Figure legend on next page

**Figure 3: Model of the mechanism of inhibition of protein synthesis in the tRip-KO parasite and consequences for timely egress of merozoites at the blood stage.** In WT parasites, the asparagine-rich C-terminal domains of *Plasmodium* CAF-1 and PABP-3 are efficiently translated by additional $tRNA^{Asn}$ provided by tRip-mediated tRNA import from the host. Full-length CAF-1 can thus down-regulate specific mRNAs including those involved in egress and invasion that adequately control parasite development. On the contrary, in the tRip-KO parasite, translation of the C-terminal domains of CAF-1 and PABP-3 is hindered by the absence of host $tRNA^{Asn}$. The delay in translation can lead to frameshifting and the occurrence of stop codons. Such a mismatch may help the stalled ribosome population to be released from the mRNA, since in the *Plasmodium* AT-rich mRNAs non-decoded asparagine codons will be shortly followed by a stop codon in the new reading frame. The resulting ΔC-CAF-1 protein can no longer regulate the translation of genes involved in parasite egress/invasion leading to early release of infectivity-deficient immature merozoites. Genes up-regulated in both mutants are highlighted in orange, they correspond to roptry-associated proteins 1, 2 and 3 (RAP1, PF3D7_1410400/PBANKA_1032100; RAP2/3, PF3D7_0501600/0501500, PBANKA_1101400), apical membrane antigen (AMA1, PF3D7_1133400/PBANKA_0915000) and merozoite surface protein 1 (MSP1, PF3D7_0930300/PBANKA_0831000).Up-regulated genes involved in merozoite's egress either in *P. falciparum* ΔC-CAF1 mutant or *P. berghei* tRip-KO parasite are listed inside green boxes: genes not in common between both strains are indicated in black: merozoite surface protein 2 (MSP2, PF3D7_0206800), glidosome associated protein 50 (GAP50, PF3D7_0918000/PBANKA_0819000), high molecular weight rhoptry proteins 2 and 3 (RhopH2, PF3D7_0929400/PBANKA_0830200 and RhopH3, PF3D7_0905400/PBANKA0416000) and Rhoptry neck protein 2 (RON2, PBANKA_1315700); Ten genes were up-regulated in the ΔC-CAF-1 mutant but were not detectable in blood stages proteomes. They are not shown on the figure; they correspond to: erythrocyte binding antigens 140, 175 and 181 (EBA140, PF3D7_1301600; EBA175, PF3D7_0731500; EBA181, PF3D7_0102500), 6-cysteine proteins P12 and P38 (PF3D7_0612700 and PF3D7_0508000), glideosome-associated protein 45 (GAP45, PF3D7_1222700), myosin A-tail interaction protein (MTIP, PF3D7_1246400/PBANKA_1459500), myosin A (MyoA, PF3D7_1342600), subtilisin-like protease 1 (SUB1, PF3D7_0507500) and calcium-dependent protein kinase 5 (CDPK5, PF3D7_1337800).

**Can host tRNAs be detected inside WT parasites and be aminoacylated by the parasite aaRSs?** To date, the import of exogenous tRNA has been demonstrated at the sporozoite stage *in vitro*, only. In blood, both reticulocytes (about 2%) and mature red blood cells (RBC) can be infected by *Plasmodia*. While reticulocytes are characterized by a dynamic protein synthesis, RBC are hyper-specialized anucleate cells taht retain about 10 % of the protein synthesis observed in reticulocytes (11). RNAs purified from mouse blood and liver have the same profile, however, the purification yield indicates that RBCs contain about 100 times less RNA than liver cells do (Figure S4A). Several human tRNAs were specifically detected by Northern Blots (Figure S4B and S5A). In a second part of the study,

Northern Blots were performed on RNA samples purified from infected blood. The profiles of the RNA samples from blood cells infected by WT *versus* tRip-KO parasites are similar, but different from that of

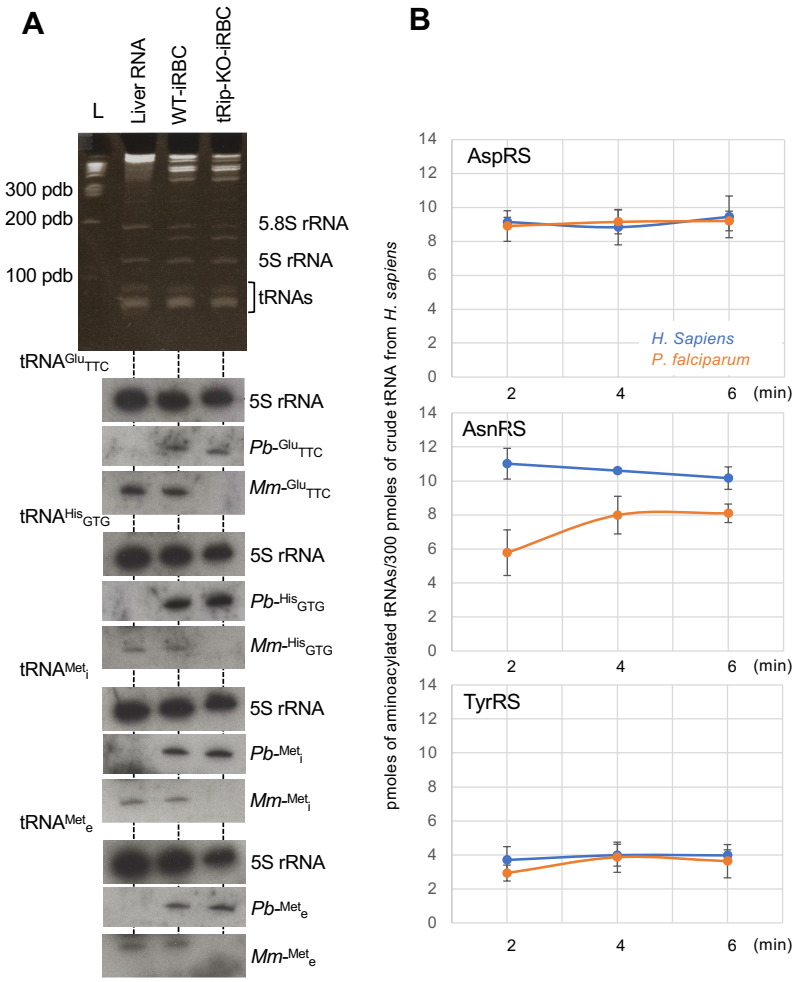


**Figure 4: Detection of host tRNAs in WT parasites and cross aminoacylation of host tRNAs by the parasite aminoacyl-tRNA synthetases.** (**A**) One µg of total RNA from the liver of non-infected (mice and 1 µg of total RNA from WT and KO parasites were analyzed on a ethidium bromide-stained 12% denaturing analytical gel. L corresponds to a DNA ladder. Northern blots experiments were completed with either probes designed to detect *P. berghei* tRNAs (*Pb*-$^{Glu}_{TTC}$, *Pb*-$^{His}$, *Pb*-$^{Met}_{i}$ and *Pb*-$^{Met}_{e}$ ) or *M. musculus* tRNAs (*Mm*-$^{Glu}_{TTC}$, *Mm*-$^{His}$, *Mm*-$^{Met}_{i}$ and *Mm*-$^{Met}_{e}$) (Figure S5). The four tRNAs belong to the category of tRNAs that interact most strongly with tRip *in vitro* (Cela et al., 2021). Detection of *Mm* tRNAs by Western blots necessitated extensive washing and long exposure of the films. (**B**) Comparative aminoacylation plateaus. Six aaRSs, aspartyl-, asparaginyl- and tyrosyl-tRNA synthetases from *H. sapiens* (in blue) or *P. falciparum* (in orange) were tested with crude human tRNAs under the same experimental conditions (6 µM crude tRNA and 0.2 µM aaRSs). Aminoacylation plateaus were measured at 2, 4, 6 min of incubation. Human crude tRNAs are potentially transcribed from 420 genes, amongst which 19 genes encode tRNA$^{Asp}$, 34 genes encoding tRNA$^{Asn}$ and 15 genes encoding tRNA$^{Tyr}$ (Chan and Lowe 2016). Error bars represent the standard deviation (SEM) of three independent experiments.

mouse RNA (Figure 4A). Four membranes were prepared with mouse liver RNA (positive control) and RNA from blood infected with the WT or the tRip-KO parasites. These samples were tested with probes designed to specifically discriminate mouse from parasite for the $tRNA^{Glu}_{TTC}$, $tRNA^{His}_{GTG}$, $tRNA^{Met}_{i}$, and $tRNA^{Met}_{e}$ isoacceptors (Figure S5B). Probes directed specifically against *P. berghei* tRNAs indicate that both parasite forms (WT and tRip-KO) contain equivalent amounts of endogenous tRNAs, as expected. In contrast, the probes designed specifically against mouse tRNAs (Figure S5A) demonstrate the presence of mouse tRNAs in liver (positive control) and in the WT parasite, indicating that the wild-type parasite imports host tRNAs. Despite the loading controls (5S rRNA) showing that the RNA deposits are comparable, mouse tRNAs were not detected in the tRip-KO parasite (Figure 5A), indicating that, tRip is essential for tRNA import

Finally, cross-aminoacylation reactions were tested using the aspartyl-, tyrosyl-, and asparaginyl-tRNA synthetases from *H. sapiens* and *P. falciparum in vitro* to determine their ability to aminoacylate human $tRNA^{Asp}$, $tRNA^{Tyr}$, and $tRNA^{Asn}$, respectively using crude human crude tRNA (Figure 4B). All three *Plasmodium* aaRSs can aminoacylate nearly the same level of tRNA as their human counterparts, although asparaginylation by the parasite enzyme is effective on about 80% of human $tRNA^{Asn}$ isodecoders. It indicates that host tRNAs, when imported into parasites by tRip can be aminoacylated by parasite aaRSs to be used in protein translation.

## Discussion

To achieve efficient and specific protein synthesis, codon usage of mRNA must be balanced with the availability of corresponding aminoacylated tRNAs in the cell (i.e.(12–15). Any discrepancy can affect the rate of protein elongation in ribosomes and result in pauses in translation that lead to mRNA degradation (16). Here, by comparing the proteomes of wild-type and tRip-KO *P. berghei*, we observe in two independent experiments that down-regulated proteins in the tRip-KO parasite are asparagine-rich proteins. Asparagine is the most used amino acid in the *P. berghei* proteome and is often found in long homorepeats (17, 18). This asparagine abundance is also found in *P. falciparum*, *P. chabaudi*, *P. yoelii* and to a lesser extent in *P.knowlesi* and *P. vivax* (Figure S3A), however proteins in the latter two parasites do not contain long asparagine repeats.

Based on our results, we propose that the absence of tRNA import in the tRip-KO parasite would prevent the accumulation of host $tRNA^{Asn}$ in the parasite and would thus explain why asparagine-rich

proteins are poorly translated. This hypothesis is strongly supported by several observations: (i) asparaginyl- and lysyl-tRNA synthetases (NRS: *p-value* = 0.063 and KRS) are overexpressed in the proteomes of tRip-KO schizonts (Figure 2A, Table S1). Both aaRSs aminoacylate tRNAs that are most used to synthesize *P. berghei* proteins. In general, increased expression of aminoacyl-tRNA synthetase is the result of a decrease in cognate aminoacyl-tRNA (19, 20). This observation suggests, that $tRNA^{Asn}$ and $tRNA^{Lys}$ levels are not high enough for efficient translation in tRip-KO schizonts. The distribution of lysines in parasite proteins is more homogeneous than that of asparagines such that the depletion of $tRNA^{Lys}$ should not affect translation as much as that of $tRNA^{Asn}$. (ii) Furthermore, mammalian (human) $tRNA^{Asn}$ is among the tRNAs with the highest affinity for *P. falciparum* tRip, along with $tRNA^{Ser}_{AGA}$ and $tRNA^{Leu}_{hGA}$ ((2), Figure 1); It is reasonable to assume that the tRNAs with the highest affinity for tRip are also those that are most efficiently imported into the parasite. (iii) Finally, compensation for low $tRNA^{Asn}$ by tRip-mediated tRNA import is only possible if the host $tRNA^{Asn}$ is a substrate for the parasite AsnRS. This is indeed the case (Figure 4B) indicating that once in the parasite, at least some host tRNA isoacceptors can be efficiently aminoacylated and used in parasite mRNA translation. Thus, some proteins down-regulated in the tRip-KO parasite would be the consequence of low $tRNA^{Asn}$ concentration that impedes their synthesis; in wild-type parasite, the selective import of $tRNA^{Asn}$ would increase its abundance in the WT parasite and play an essential role in the decoding of asparagine-rich proteins.

In the present study, despite several attempts, we were unable to design specific probes that could efficiently differentiate human from parasite $tRNA^{Asn}$ (Figure S5B). However, a non-specific Northern Blot probe hybridizing both endogenous parasite tRNAs and imported host tRNAs showed that, despite their excessive use in protein translation, *P. falciparum* $tRNA^{Asn}$ does not accumulate more than other tRNAs in the blood stages of the parasite (21). This observation is in line with our hypothesis that insertions, and especially asparagine-rich insertions, could regulate ribosome translation rates and influence protein co-translational folding (22, 23). Here, we propose that the import of host $tRNA^{Asn}$ enables the decoding of such asparagine-rich sequences. These two scenarios can coexist, if $tRNA^{Asn}$ import remains moderate. Both mechanisms of translational regulation depend on how much $tRNA^{Asn}$ is available to decode asparagine-rich sequences, as long as the $tRNA^{Asn}$ concentration remains limited to slow down ribosomal translation locally to facilitate protein folding.

Two asparagine-rich proteins stand out and are conserved in the six *Plasmodium* species analyzed (Table S5): the CCr4-associated factor 1 (CAF-1), involved in the poly-(A) decay of mRNAs

(24), and to the poly-(A) binding protein-3 (PABP3), which has not yet been characterized in *Plasmodium*. Not only are both proteins involved in poly-(A) recognition, but they also adopt a common global structure with highly conserved N-terminal domain sequences and a C-terminal domain found only in *Plasmodia* with very high asparagine content. The conserved N-terminal domain of CAF-1 is essential for the decay of mRNAs enriched in non-optimally decoded codons; it belongs to the eukaryotic CCr4-Not complex, which binds to the empty E-site of the ribosome and properly positions CAF-1 to initiate the decay of the 3′-poly(A)-tails of stalled mRNAs (25). Interestingly, the deletion of the C-terminal sequence of *Plasmodium* CAF-1 is not essential and leads to the premature release of non-infectious merozoites *in vitro* (10) and the inappropriate development of gametocytes involved in transmission from host to vector *in vivo* (26). Here, in the absence of tRip-mediated tRNA import, the asparagine-rich C-terminal domain of CAF-1 (and of PABP-3) would remain untranslated, leading to parasites with low invasion capacities. Indeed, disruption of tRip and of the C-terminal domain of CAF-1 not only lead to the same phenotype: parasites have reduced infectivity and multiplication in the blood stage (1, 10), but also results in overexpression of the same gene products involved in invasion (Table S3, Figure 3).

In conclusion, the complex life cycle of *Plasmodium* is highly regulated and involves tight transcriptional and especially post-transcriptional controls (27, 28). In this study, host tRNAs imported by tRip would ensure correct translation of asparagine-rich protein domains, including the C-terminal domains of CAF-1. This domain tightly controls the expression of mRNAs encoding proteins responsible for the release of mature merozoites and thus ensures efficient infection and parasite development in the blood (Figure 3). The amount of tRNA in RBC is small and yet sufficient to be imported inside the wild-type parasite (Figure 4A). It is interesting to note that blood also contains reticulocytes, which are precursors of RBCs very active in translation and therefore rich in tRNAs (Smith and McNamara, 1972). Despite the rarity of these reticulocytes in blood (about 2% of blood cells), *P. berghei* (29), *P.chabaudi* (30), *P. yoelii* (31) and *P. vivax* (32) preferentially invade these cells compared to mature RBCs. In addition, variations in tRNA isodecoder expression and post-transcriptional modifications between tissues (33, 34), represent diverse sources of exogenous tRNAs that may differentially control parasite translation profiles and enable efficient stage transitions not only in the vertebrate blood or liver but also in mosquitoes. In such model, variations in tRNA, and especially $tRNA^{Asn}$, supply could play a major role in parasite development by modulating the translational efficiency of certain mRNAs, further supporting the of “just-in-time” translation model (27).

## Material and Methods

**Parasite production:** Four- to six-week-old female mice (C57BL/6), weighing approximately 20 g, were injected intraperitoneally with 200 µL of frozen infected red blood cells (10-15% parasitemia diluted in phosphate-buffered saline (PBS)) either with wild-type (WT, *Pb* gfpGOMO14) or with tRip-KO (*Pb* tRip-KO mCherry) malaria parasites derived from the *P. berghei* (ANKA strain). Parasitemia was monitored daily by cytometry (BD Accuri C6). Mice with parasitemia between 5 and 10% were selected for testing. Therefore, in this study, only mice without or low symptoms were used. These parasitemia levels were reached 3-6 days after parasite injection. Mice were put to sleep and blood was collected by intracardiac puncture (about 1 to 1.5 mL) and parasites were directly purified (all blood stages) or cultured for 24 hours in RPMI at 37°C under 5% CO2 (only schizonts).

infected blood was filtered through a Plasmodipur filter (Europroxima) to remove mouse leukocytes, centrifuged for 10 min at 450 g and recovered in 4 mL of RPMI. A 7.2 mL cushion of 60% isotonic Percoll was gently pipetted under the red blood cells and the tube was centrifuged for 20 min at 1450 g (swinging buckets), to separate infected red blood cells (iRBC) at the Percoll/RPMI interface from non-infected RBC at the bottom of the tube. Parasitized RBCs were recovered in 2 tubes, washed 3 times in 1 mL of PBS and combined with 200 µL each of PBS. Infected RBCs were then lysed with 0.02% saponin for 5 min in ice (in 400 µL). Free parasites were recovered by centrifugation for 5 min at 2000 g and washed in 500 µL of PBS. The two pellets were resuspended either in 50 µL of protein loading buffer and stored at -80°C until mass spectrometry analysis, or as is and placed at -80°C for RNA preparation. All experiments were performed in accordance with relevant guidelines and regulations under the project license for animal experimentation #11124-2018010312571506.

**Mass spectrometry (MS) and data analyses**. Approximately 10 µg of protein was obtained from the half of the blood (~0.75 mL of a 5-10% infected mouse). Protein concentrations were determined by Bradford assay using bovine serum albumin as the standard. Proteins were precipitated, reduced, and alkylated as described in (3). After digestion overnight with sequencing grade porcine trypsin (300 ng, w/w, Promega, Fitchburg, MA, USA), the generated peptides were analyzed either using Easy-nanoLC-1000 system coupled to a Q-Exactive Plus mass spectrometer (Thermo Fisher Scientific, Germany) with 160-minutes gradients (blood stages) or a NanoLC-2DPlus system (nanoFlexChiP module; Eksigent, ABSciex, Concord, Ontario, Canada) coupled to a TripleTOF 5600 mass spectrometer (ABSciex) operating in positive mode with 120-minutes gradients (schizonts). Data were searched using the

Mascot algorithm (version 2.6.2, Matrix Science) against the Uniprot database with *P.Berghei* taxonomy (release 2021_03, 4 927 sequences) with a decoy strategy. The resulting .dat Mascot files were then imported into Proline version 2.0 software (35) to align the identified proteins. Proteins were then validated with Mascot pretty rank equal to 1, and 1% false discovery rate (FDR) on both peptide spectrum matches (PSM) and protein sets (based on Mascot score).

For statistical analyses, raw Spectral Count values were imported into R (v. 3.5.0) where the number of spectra were first normalized using the DESeq2 median of ratio normalization method. A negative-binomial test using an edgeR GLM regression generated for each identified protein a p-value and a protein fold-change (FC). The R script used to process the dataset is published on Github (36). Proteins were statistically enriched or decreased with a p-value < 0.05 and a minimum fold change (FC) of 2 or 0.5, respectively. Mass spectrometry proteomic data will be deposited within the ProteomeXchange Consortium via the PRIDE partner repository (37) with the dataset ID PXD043916.

**Northern blots.** Infected red blood cell (iRBC) pellets were incubated in 2 mL of cold lysis buffer (10 mM $KHCO_3$, 150 mM $NH_4Cl$ and 0.1 mM EDTA) for 15 min on ice. Cellular debris was removed by centrifugation for 5 min at 100 g and parasites were recovered by centrifugation of the supernatant for 5 min at 6000 g. Parasites were then washed three times in 2 mL of PBS. Northern blots were performed, using $^{32}P$-labeled DNA probes designed to detect *Mus musculus* (*Mm*) tRNAs in RBCs or differentiate *P. berghei* (*Pb*) from *Mm* tRNAs in iRBCs (Figure S5). One µg or 5 µg of total RNA (from *Mm* Liver, RBCs or iRBCs) were separated on a 12% acrylamide/bisacrylamide (19 :1), 8 M urea, 1 x TBE denaturing gel. RNAs were transferred to a positively charged nylon membrane (BrightStarTM Plus, Ambion) at 200 mA for 30 min and crosslinked for 2 min at 120 mJ (Stratagen). Membranes were pre-incubated for 2 h at 60ºC and hybridized overnight at 60ºC in hybridization buffer (UltraSensitive Buffer, Ambion) with $3.10^6$ cpm of radioactive probe. Membranes were rinsed and washed twice for 20 min at 60ºC with 5 mL of 2X SSC (300 mM sodium chloride and 34 mM sodium citrate, 0.1% SDS). This protocol was conducted twice in a row first with the tRNA probes and second with the common 5S rRNA probe before being exposed to a high-resolution film (Carestream).

## Aknowledgments

We are grateful to Philippe Hammann, Lauriane Kuhn, and Béatrice Chane Woon Ming for LC-MS/MS analysis, Fabrice Auge and Eric Marois for animal experiments, and to Dr Alain Lescure and

Prof Tamara Hendrickson for providing comments on this manuscript. This work was performed under the framework of the Interdisciplinary Thematic Institute IMCBio, as part of the ITI 2021-2028 program of the University of Strasbourg, CNRS and Inserm. It was supported by IdEx Unistra (ANR-10-IDEX-0002), by SFRI-STRAT'US project (ANR 20-SFRI-0012), and EUR IMCBio (IMCBio ANR-17-EURE-0023) under the framework of the French Investments for the Future Program, by previous Labex NetRNA (ANR-10-LABX-0036), by the CNRS and the Université de Strasbourg, IdEx "Equipement mi-lourd" (2015) and Equipement d'Excellence (EquipEx) I2MC (ANR-11-EQPX-0022), and by the Fondation pour la Recherche Médicale (FRM) (grant number FDT201704337050) to Marta Cela.

## References

1. T. Bour, *et al.*, *Apicomplexa*-specific tRip facilitates import of exogenous tRNAs into malaria parasites. *Proc Natl Acad Sci USA* **113**, 4717–4722 (2016).

2. M. Cela, *et al.*, Identification of host tRNAs preferentially recognized by the *Plasmodium* surface protein tRip. *Nucleic Acids Research*, gkab769 (2021).

3. J. R. Jaramillo Ponce, D. Kapps, C. Paulus, J. Chicher, M. Frugier, Discovery of two distinct aminoacyl-tRNA synthetase complexes anchored to the Plasmodium surface tRNA import protein. *Journal of Biological Chemistry* **298**, 101987 (2022).

4. J. R. Jaramillo Ponce, *et al.*, Solution X-ray scattering highlights discrepancies in *Plasmodium* multi-aminoacyl-tRNA synthetase complexes. *Protein Science* **32** (2023).

5. S. Gupta, *et al.*, Crystal structures of the two domains that constitute the *Plasmodium vivax* p43 protein. *Acta Crystallogr D Struct Biol* **76**, 135–146 (2020).

6. K. Deinert, F. Fasiolo, E. C. Hurt, G. Simos, Arc1p organizes the yeast aminoacyl-tRNA aynthetase complex and stabilizes its interaction with the cognate tRNAs. *Journal of Biological Chemistry* **276**, 6000–6008 (2001).

7. A. M. Minns, K. J. Hart, S. Subramanian, S. Hafenstein, S. E. Lindner, Nuclear, cytosolic, and surface-localized Poly(A)-binding proteins of *Plasmodium yoelii*. *mSphere* **3** (2018).

8. S.-J. Cha, M.-S. Kim, A. Pandey, M. Jacobs-Lorena, Identification of GAPDH on the surface of *Plasmodium* sporozoites as a new candidate for targeting malaria liver invasion. *Journal of Experimental Medicine* **213**, 2099–2112 (2016).

9. C. Aurrecoechea, *et al.*, ApiDB: integrated resources for the apicomplexan bioinformatics resource center. *Nucleic Acids Research* **35**, D427–D430 (2007).

10. B. Balu, *et al.*, CCR4-Associated Factor 1 Coordinates the Expression of *Plasmodium falciparum* egress and invasion proteins. *Eukaryot Cell* **10**, 1257–1263 (2011).

11. S. D. Kumar, *et al.*, Evidence for low-level translation in human erythrocytes. *MBoC* **33**, br21 (2022).

12. E. M. Novoa, L. Ribas de Pouplana, Speeding with control: codon usage, tRNAs, and ribosomes. *Trends in Genetics* **28**, 574–581 (2012).

13. J. D. Richter, J. Coller, Pausing on polyribosomes: Make way for elongation in translational control. *Cell* **163**, 292–300 (2015).

14. M. Torrent, G. Chalancon, N. S. de Groot, A. Wuster, M. Madan Babu, Cells alter their tRNA abundance to selectively regulate protein synthesis during stress conditions. *Sci. Signal.* **11**, eaat6409 (2018).

15. P. C. Dedon, T. J. Begley, Dysfunctional tRNA reprogramming and codon-biased translation in cancer. *Trends in Molecular Medicine* **28**, 964–978 (2022).

16. Q. Wu, *et al.*, Translation affects mRNA stability in a codon-dependent manner in human cells. *eLife* **8**, e45396 (2019).

17. S. R. Chaudhry, N. Lwin, D. Phelan, A. A. Escalante, F. U. Battistuzzi, Comparative analysis of low complexity regions in *Plasmodia*. *Sci Rep* **8**, 335 (2018).

18. F. U. Battistuzzi, *et al.*, Profiles of low complexity regions in *Apicomplexa*. *BMC Evol Biol* **16**, 47 (2016).

19. Harald Putzer, Laalami Soumaya, "Regulation of the expression of aminoacyl-tRNA synthetases and translation factors" in *Madame Curie Bioscience Database*, (Landes Bioscience, 2000).

20. O. Levi, S. Garin, Y. Arava, RNA mimicry in post-transcriptional regulation by aminoacyl tRNA synthetases. *WIREs RNA* **11** (2020).

21. D. Filisetti, *et al.*, Aminoacylation of *Plasmodium falciparum* $tRNA^{Asn}$ and Insights in the synthesis of asparagine repeats. *Journal of Biological Chemistry* **288**, 36361–36371 (2013).

22. M. Frugier, *et al.*, Low Complexity Regions behave as tRNA sponges to help co-translational folding of plasmodial proteins. *FEBS Lett* **584**, 448–54 (2010).

23. Y. Wang, H. J. Yang, P. M. Harrison, The relationship between protein domains and homopeptides in the *Plasmodium falciparum* proteome. *PeerJ* **8**, e9940 (2020).

24. M. A. Collart, The Ccr4-Not complex is a key regulator of eukaryotic gene expression. *WIREs RNA* **7**, 438–454 (2016).

25. R. Buschauer, *et al.*, The Ccr4-Not complex monitors the translating ribosome for codon optimality. *Science* **368**, eaay6912 (2020).

26. K. J. Hart, *et al.*, *Plasmodium* male gametocyte development and transmission are critically regulated by the two putative deadenylases of the CAF1/CCR4/NOT complex. *PLoS Pathog* **15**, e1007164 (2019).

27. S. S. Vembar, D. Droll, A. Scherf, Translational regulation in blood stages of the malaria parasite *Plasmodium spp.* : systems-wide studies pave the way: Translational regulation in blood stages of the malaria parasite. *WIREs RNA* **7**, 772–792 (2016).

28. S. Bennink, G. Pradel, The molecular machinery of translational control in malaria parasites. *Mol Microbiol* **112**, 1658–1673 (2019).

29. D. Cromer, K. J. Evans, L. Schofield, M. P. Davenport, Preferential invasion of reticulocytes during late-stage *Plasmodium berghei* infection accounts for reduced circulating reticulocyte levels. *International Journal for Parasitology* **36**, 1389–1397 (2006).

30. R. Antia, A. Yates, J. C. De Roode, The dynamics of acute malaria infections. I. Effect of the parasite's red blood cell preference. *Proc. R. Soc. B.* **275**, 1449–1458 (2008).

31. B. Mons, Preferential invasion of malarial merozoites into young red blood cells. *Blood Cells* **16**, 299–312 (1990).

32. N. Thawani, *et al.*, Plasmodium Products Contribute to Severe Malarial Anemia by Inhibiting Erythropoietin-Induced Proliferation of Erythroid Precursors. *The Journal of Infectious Diseases* **209**, 140–149 (2014).

33. K. A. Dittmar, J. M. Goodenbour, T. Pan, Tissue-specific differences in Human transfer RNA expression. *PLoS Genet* **2**, e221 (2006).

34. O. Pinkard, S. McFarland, T. Sweet, J. Coller, Quantitative tRNA-sequencing uncovers metazoan tissue-specific tRNA regulation. *Nat Commun* **11**, 4104 (2020).

35. D. Bouyssié, *et al.*, Proline: an efficient and user-friendly software suite for large-scale proteomics. *Bioinformatics* **36**, 3148–3155 (2020).

36. L. Kuhn, T. Vincent, P. Hammann, H. Zuber, "Exploring Protein Interactome Data with IPinquiry: Statistical Analysis and Data Visualization by Spectral Counts" in *Statistical Analysis of Proteomic Data*, Methods in Molecular Biology., T. Burger, Ed. (Springer US, 2023), pp. 243–265.

37. Y. Perez-Riverol, *et al.*, The PRIDE database resources in 2022: a hub for mass spectrometry-based proteomics evidences. *Nucleic Acids Research* **50**, D543–D552 (2022).

# Supporting Information

## SI Materials and Methods

**Bioinformatics.** Protein sequences as well as proteomes from all *Plasmodium* strains were retrieved from PlasmoDB. A home-made Python 2.7 script was used to calculate the asparagine content for each protein sequence. *Toxoplasma gondii* was the outgroup species.

**RNA purification and QRT-PCR.** Total RNA was extracted from parasites using the RNeasy Mini Kit (Qiagen) according to the manufacturer's protocol and was subjected to DNAse treatment with the Rapid OUT DNA removal kit (Thermo Scientific). Total RNA was analyzed and quantified on Bioanalyser (puce PICO). Each sample was reverse transcribed in a 20 µL reaction volume containing 10 µL (0.16 to 0.5 µg) of RNA, using the SuperScript II reverse transcriptase (Invitrogen) according to the manufacturer's protocol. The mRNAs levels were measured by RT-PCR (25 µL containing 4 µL of cDNA) on a CFx94 (Bio-Rad) using the Syber Green kit (Thermo Scientific). Oligonucleotides used for qRT-PCR are listed in Table S4. qRT-PCR reactions were designed according MIQE guidelines (Bustin et al. 2009), the specificity of the oligonucleotides was validated, and the amplification efficiencies of the primer sets are all between 90 and 110% and $r^2$ values greater than 0.96. The mRNAs levels were calculated according to the $\Delta$Cq method and normalized by the mRNA level of both the EF1-$\alpha$ and Hsp70 in each sample. Raw data are indicated as mean of three measurements, and results were expressed as the average of 3 biological samples ± standard error of the mean (SEM).

**Purification of aminoacyl-tRNA synthetases and aminoacylation assays.** Recombinant *P. falciparum* and *H. sapiens* NRS and DRS were cloned, expressed and purified as described in references (Filisetti et al. 2013; T. Bour et al. 2009) respectively. The gene encoding the *P. falciparum* TyrRS was amplified by PCR from *P. falciparum* cDNA and cloned into pQE30 (Qiagen) and the plasmid encoding the *H. sapiens* YRS was a gift from P. Schimmel. Both *P. falciparum* and *H. sapiens* YRS were expressed and purified as described for NRS (Filisetti et al. 2013). Purified enzymes are shown in Fig S4C. *H. sapiens* crude tRNAs was prepared as described in (Cela et al. 2021).

Aminoacylation assays were performed under the same conditions: at 37 °C for 2, 4 and 6 min in 50 mM HEPES-KOH (pH 7.5), 20 mM KCl, 10 mM $MgCl_2$, 2 mM ATP, 6 μM total tRNA from HeLa cells, in the presence of 20 μM of the corresponding L-[$^{14}$C]-amino acid (Perkin Elmer). AaRSs were diluted in 100 mM HEPES-KOH pH 7.5, 1 mM DTT, 5 mg/mL BSA, and 10% glycerol and used at a final concentration of 200 nM in the aminoacylation assay. The aminoacylation plateaus are the mean of 3 independent experiments ± standard deviation (SD).